INTRODUCTION AND SENSITIVITY ANALYSIS OF FILLING PROCESS OF VISCOUS TORSIONAL VIBRATION DAMPER

Márk VENCZEL[1] and Árpád VERESS[1,2]

[1]Department of Aeronautics and Naval Architecture
Faculty of Transportation Engineering and Vehicle Engineering
Budapest University of Technology and Economics
H-1111 Budapest, Hungary

[2]Knorr-Bremse R&D Center Budapest, Engineering Calculations, Major u. 69,
H-1119, Budapest, Hungary

Received: November 11, 2020

ABSTRACT

While the downsizing, down-speeding and turbo-supercharging design trends prevail in the internal combustion engine market nowadays, the crankshafts are exposed to harmful torsional oscillations originated from the increased torque and lightweight structure. To avoid the fatigue damage of the crankshaft and the engine components, caused by the unwanted torsional vibrations, viscous torsional vibration dampers (shortly visco-dampers) are mounted onto the free end of the crankshaft or integrated into the flywheel. The working fluid of this kind of vibration damper is a high viscosity non-Newtonian silicone fluid. The reduction of manufacturing time is a key factor for increasing productivity by having shorter time frame required for the silicone oil to be filled into the narrow damper gap channels. The filling time depends strongly on the filling conditions which must be investigated in detail with considering the degradation-free processes. The aim of the present work is to provide and insight into the filling process of visco-dampers with considering the absolute pressure and dynamic viscosity distributions in the damper gap geometry and to analyse the impact of the applied inlet overpressure, oil temperature and the slope of pressure ramp-up onto the filling time in numerical way. The parameter sensitivity analyses have been performed with six different inlet overpressures, four different oil temperatures and four different slopes of inlet pressure ramp-up by 3D transient, multiphase, coupled fluid dynamic and heat transfer simulations in ANSYS FLUENT fluid dynamic software. The identification of the most influencing boundary condition on the filling time is the outcome of present work.

Keywords: torsional vibration damper, silicone fluid, dynamic viscosity, CFD, parameter sensitivity analysis

1. INTRODUCTION

The torsional vibration and the fatigue damage of the crankshaft became a prominent problem at the internal combustion engine of sea ships from the late 1800s. Based on the statistics, between 1882 and 1885 the shaft of 228 ships were already broken and this number started increasing by the appearance of diesel-powered ocean liners [1]. In early designs the torsional oscillations arising on the shafts could not be recognized, well understood and properly controlled. Designers explained the broken crankshaft with the fact, that the damaged engine component was not sized properly for the desired amount of torque to carry based only on gas pressure and inertia force calculations. Vibratory loads were totally neglected. At the beginning of the 19th century, several researches were launched to find out the cause of the problem. Lorenz [2] in his book, published in 1901, analysed the dynamics of the crankshaft of ships. In 1902, H. Frahm's work [3] on the problem of shaft fractures was published. A series of publications dealing with the problem of torsional vibration of drives was opened by G. W. Melville (1903) and S. P. Timoshenko (1905). [4] [5]

1.1 Torsional oscillations on the crankshaft of internal combustion engines

As presented in Fig. 1 (left), by burning fuel in engine cylinders, thermal energy is released and converted into mechanical load (torque) through the pistons and connecting rods of the crankshaft. The periodically varying gas forces and the unbalanced running of rotating masses of the shaft induce continuous repetition of momentary angular acceleration ruled by the ignition and injection sequence. This motion leads to irregular and periodic vibrations on the crankshaft which are transferred to other engine components through the drive belt and timing chain. As a result, significant mechanical stresses arise in the drivetrain. These unwanted oscillations tend to reduce engine power, increase fuel consumption and are responsible for noise and engine failure. In case the frequency of the oscillation corresponds to the natural frequency of the crankshaft and driven components, fatigue damage occurs. [6] Nowadays, downsizing, down-speeding and turbo-supercharging design trends prevail in the internal combustion engine market which can further exacerbate the above-mentioned vibration problems by causing increased torque on the crankshaft. [7]

1.2 Viscous torsional vibration dampers

An opportunity to prevent the crankshaft from fatigue damage caused by torsional oscillations is to eliminate the amplitude of vibrations by mounting a viscous torsional vibration damper (visco-damper) onto the free-end of the crankshaft (see left side of Fig. 1) or by integrating it into the flywheel.

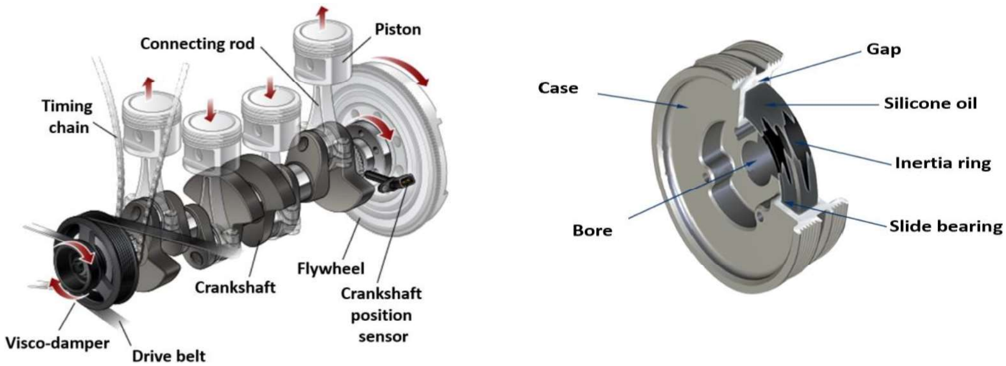

Fig. 1 Crankshaft configuration (left) and structure of a visco-damper (right) [8]

Visco-damper consists of a closed annular space, called case, with a freely moving inertia ring enclosed in it according to Fig. 1 (right). The inertia ring is guided by polymer slide bearings and surrounded by a thin film of silicone oil. The operation and the damping process can be explained as follow. Provided that there is only undisturbed rotation of the crankshaft without superposed oscillations, the inertia ring rotates together with the case without any slip. As torsional oscillations appear on the shaft, the damper case (fixed to the rotating crankshaft) begins in relative motion to the inertia ring and tangential shear stress occurs in the silicone fluid. The damping effect is the sum of the shear stresses developing on the friction surfaces between the case and the inertia ring. Silicone oil is a non-Newtonian, viscoelastic and shear-thinning (higher shear rate makes the fluid more fluent) fluid and it has a different response to external forces compared to other conventional (Newtonian) fluids. Because of these characteristics, the relative velocity between the case and the inertia ring affects the viscosity and thus the damping characteristics of the oil. During operation, the damping fluid can be exposed to high thermal load originating from the shear and friction of the oil layers and from the engine and surrounding air. The viscosity of the silicone oil (and thus the damping characteristics of the oil) varies with the change in temperature. By loading the oil to extreme (high) temperatures, overheating, degradation can occur together with reduction of damping effect and the oil turns into black colour (see left side of Fig. 2). To keep the operational temperature within the designed range, cooling fin plates may be mounted onto the case as shown in Fig. 2 (right). [9]

Fig. 2 Degradation levels in silicone oil samples (left) and cooling fins on visco-damper (right) [10] [9]

1.3 Application and filling process of visco-dampers

Visco-dampers have a wide range of application fields from high power reciprocating engine of vehicles through energetics to the mining sector of industry. They are applied not only in automotive, aircrafts, marine, combined heat and power, industrial manufacturing & processing sectors, but in energy, utilities, landfill, biogas and agriculture areas as well [11]. Considering the above-listed wide field of use, the manufacturing process of this damping product must be highly productive, immediate and continuous.

As the final step of the manufacturing process of visco-dampers, the damper gap is filled with silicone oil by using a specific filling machine. During the filling process, the oil enters the filling chamber, which is formed in the inertia ring and found just below the inlet, through an inlet hole with diameter smaller than 10 mm. Because of the highly viscous nature of the oil, the small size of the hole and the narrow dimensions of the gap (bounded by the internal surfaces of the case and outer surfaces of the inertia-ring and bearings) filling can take long time. [12]

Silicone oil can suffer from thermal and mechanical load during the filling process. Hence, the filling conditions must be controlled to reach minimal filling time by avoiding permanent and unrecoverable viscosity loss (called mechanical and thermal degradation of the molecular chains). Based on these facts, the aim of the present paper is to reveal the flow characteristics of the filling process, to investigate the possibilities of filling time reduction on a conceptual visco-damper gap geometry and to perform sensitivity analysis to identify the most influencing parameters on the filling time.

2. APPLIED NUMERICAL METHOD

2.1 Computational Fluid Dynamics

The motion of fluids (liquids and gases) and the forces on them are governed by nonlinear partial differential equations which represent the conservation of mass, momentum and energy, known as Navier-Stokes equations (see Eq. (1) in a compact and versatile form). They have been known for over 160 years, however, there is no closed-form solution of them for general flow cases up till now. Computational Fluid Dynamics (CFD) is a powerful numerical tool for engineers to replace these partial differential equations by a set of algebraic equations that can be solved by using computers. CFD, in the present application uses finite-volume-method based discretisation technique to convert the investigated flow domain into a series of control volumes, cells. The algebraic equations are then interpreted on these control volumes to calculate the flow parameters in each cell and to render the solution field. [13]

$$\frac{\partial}{\partial t}\int_V \rho\Phi dV + \oint_A \rho\Phi \boldsymbol{V}\cdot d\boldsymbol{A} = \oint_A \Gamma_\Phi \nabla\Phi\cdot d\boldsymbol{A} + \int_V S_\Phi dV\,. \qquad (1)$$

In Eq. (1) the parameters are the followings: t – time, $\boldsymbol{V}$ – domain volume, ρ – density, $\boldsymbol{A}$ – domain surface, S – source term, Γ – equation specific diffusion coefficient, ∇ – nabla operator, Φ – parameter for the type of equation. If $\Phi = 1 \rightarrow$ continuity equation, $\Phi = u \rightarrow$ momentum equation in X direction, $\Phi = v \rightarrow$ momentum equation in Y direction, $\Phi = w \rightarrow$ momentum equation in Z direction in case of Cartesian coordinate system and $\Phi = E \rightarrow$ energy equation. u, v, and w are the velocity components in the Cartesian coordinate system and E is the specific total energy.

FLUENT 2019 R1 commercial software has been used in Ansys Workbench environment to calculate the filling process on a visco-damper's gap geometry. The interface between air and silicone oil is calculated by Volume of Fluid (VOF) method. VOF is a free-surface modelling technique for two or more immiscible fluids (liquid or gas phases) that allows to track the volume fraction of each of the fluids throughout the domain in any time step by solving a single set of momentum equations. Main applications of VOF method are the prediction of jet breakup, the motion of large bubbles in a liquid or the transient tracking of any liquid-gas interface. The tracking of the interface between the phases is based on the solution of continuity equation for the volume fraction of the phases. For the q^{th} phase this equation is presented by Eq. (2) [14]

$$\frac{1}{\rho_q}\left[\frac{\partial}{\partial t}(\alpha_q\rho_q) + \nabla(\alpha_q\rho_q\vec{v}_q) = S_{\alpha_q} + \sum_{p=1}^{n}(\dot{m}_{pq} - \dot{m}_{qp})\right], \qquad (2)$$

where ρ_q – density of the q^{th} phase, t – time, α_q – volume fraction of q^{th} phase, $\vec{v}_q$ – velocity vector of the q^{th} phase, S_{α_q}– mass source term, $\dot{m}_{pq}$ – mass transfer from phase p to phase q, $\dot{m}_{qp}$ – mass transfer from phase q to phase p. In current case there is no phase transition and no source or sink, thus the right side of Eq. (2) equals to zero.

2.2 The investigated flow field and the CFD model

A conceptual visco-damper's 3D gap geometry with segment angle of 110° (see left side of Fig. 3) has been used to calculate the filling process in the transient simulations. The reason of that, instead of using the whole geometry, is to avoid long calculation time and large amount of generated result files. The gap for the silicon oil is situated in the domain bounded by the case, inertia ring and bearings. The investigated flow domain has an "U" shaped form as it is shown in the left side of Fig. 3. The outer and inner diameter of its bounding box is 165 mm and 127 mm, determined by the case and the bearings respectively. The overall thickness of the geometry in axial direction is 19 mm. The flow domain has only one plane of symmetry that passes through the filling hole. The diameter of filling hole is 5.5 mm and a 10 mm long inlet channel has been attached to the filling hole to enhance convergence in first calculation steps and to reduce the influence of inlet boundary by setting it properly far from the inlet section.
Considering the complexity of the geometry (the slot for the flow varies from a few tenths to 10 mm) and the properly fine and uniform mesh requirements of a transient simulation, the investigated domain is divided into 0.25 mm sized polyhedral elements. The final mesh, presented in Fig. 3 (right), is built up from 1,597,788 number of elements and contains 5,673,294 number of nodes. The inflation layer near the walls is divided into 3 sublayers with 0.3 transition factor and 1.35 growth rate.

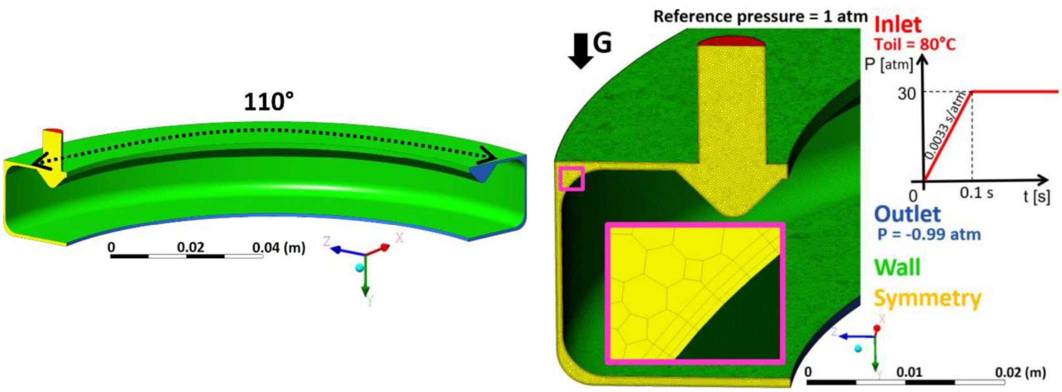

Fig. 3 The investigated flow field (left) with the numerical mesh, reference pressure, coordinate system, ruler and boundary conditions (right)

Convective heat transfer has been defined in the outside solid walls of the flow domain with the heat transfer coefficient of 8 $W/m^2/K$ with 25 °C bulk temperature based on [15]. The initial air temperature in the gap is set to 25 °C while the initial gap pressure as well as the outlet pressure is set to 0.01 atm in each simulation case. Symmetry boundary condition has been applied in the plane of symmetry.
The influence of oil total inlet temperature has been investigated at four different temperature values (25 °C, 40 °C, 60 °C and 80 °C) and the highest value has been selected as 40% of silicone oil's highest allowable temperature (200 °C) based on [16]. During analyses six different inlet overpressures (1 atm, 5 atm, 10 atm, 15 atm, 20 atm and 30 atm) have been applied for each oil temperature which follow a ramp function

described by the target pressure and ramping time (the duration, along which the target pressure is reached) as shown in Fig. 3 (right). According to [16], silicone oil's initial viscosity doubles at 450 bar, thus the highest inlet overpressure value (30 atm) in the current investigation has been selected as it is smaller than 10 % of this mentioned value to let the oil be sufficiently fluent at 25 °C. The slope of the pressure ramp is the same (0.0033 s/atm) in each pressure case. In the simulation case of 30 atm inlet overpressure with 80 °C oil temperature, the influence of the pressure ramp has been analysed by varying its slope such as 0.0011 s/atm, 0.0016 s/atm, 0.0033 s/atm, and 0.0066 s/atm values. The simulation case with 30 atm inlet overpressure, 80 °C oil temperature and 0.0033 s/atm slope of pressure ramp has been considered as reference filling simulation. The numerical results of the reference filling simulation are discussed in detail in subchapter 3.1.

The effect of the total temperature, the total pressure and the slope of the pressure ramp on the structural integrity of the silicon oil is not investigated.

The most important specific physical models, methods and parameters used in the simulation are implicit VOF method (to calculate the interface between air and silicone oil), surface tension coefficient (on the interface of air and silicone oil), contact angle (to model the wall adhesion of silicone oil), viscous heating (to model the heat generation originated from shearing of oil layers), temperature-dependent density model of silicone oil based on [16], temperature- and shear rate-dependent Carreau-Yasuda viscosity model of silicone oil with five parameters based on [17], implicit body force treatment (to make the solution more robust by taking into account the effect of body forces and partial equilibrium pressure gradient caused by gravity).

The filling process analysis is stopped, in the recent case, when the silicone oil runs around in the arc of 110° flow domain and reaches the outlet. The oil velocity shows monotonically decreasing trend (see right side of Figs. 4 – 6), which results longer simulation time and more data. This confirms the need for the reduced-size flow domain. Converged results have been gained in each simulation case as the residuals of mass, momentum and oil volume fraction are below 1E-5 while the residual of the energy converges below 1E-8 at the end of the simulations.

3. NUMERICAL RESULTS

3.1 Filling process analysis of the reference simulation case

Left side of Figs. 4 – 6 present the absolute pressure distribution in the damper gap while the right side of the figure shows the actual position of the filled amount of silicone oil coloured by actual dynamic viscosity values. At normalized time of 0.05 the target value of inlet overpressure (30 atm) is not built up yet, however the pushing effect of the current inlet pressure and the suction effect of minimal pressure (0.01 atm) in the gap make the fluid sufficiently fluent and cause high shear rates and shear stresses in the oil to (the maximum dynamic viscosity is 92.64%). The maximum velocity is situated at the filling hole (presented with arrow on the right side of Figs. 4 – 6). As the time passes, the maximal inlet overpressure is reached at 0.1 s and due to the strong viscous behaviour of the oil, high pressure zones start spreading in the oil in a relatively slow rate respect to the flow rate of the oil front. The more amount of oil is filled into the gap the higher pressure is needed to keep the oil at constant spreading

velocity (considering the high viscous behaviour again), thus shear rates start monotonically decreasing, oil becomes more viscous and the inflow decelerates.
During the filling process, highest viscosity zones are situated along the center line of the inlet channel, at the corners of the gap and at the fluid flow front where the oil is exposed to low shear rate. At the end of the investigated filling process, a maximum viscosity increases by 48.36 % and a maximum velocity decreases by 81.68 % compared to the values recorded at the first calculated timestep.

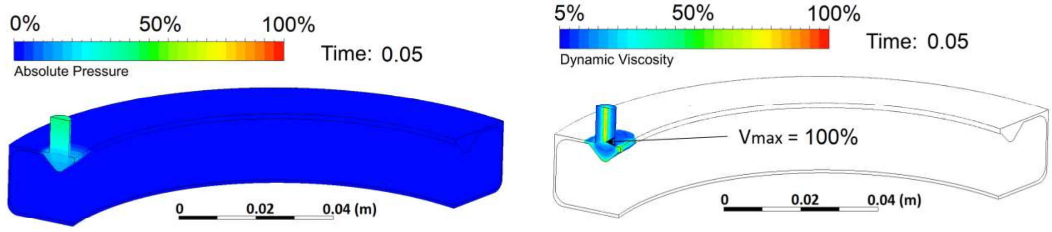

Fig. 4 Absolute pressure distribution (left) and oil spread with dynamic viscosity and maximal velocity (right) at normalized time of 0.05

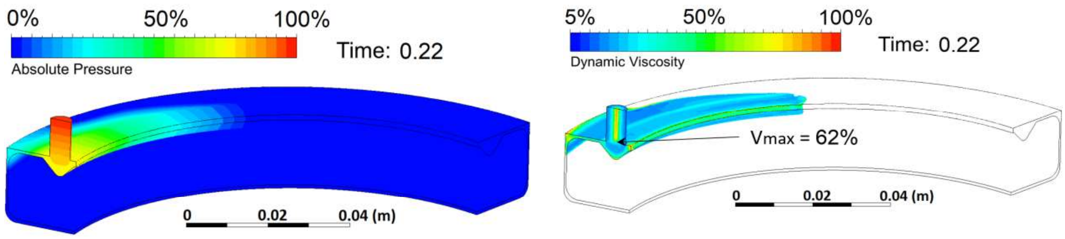

Fig. 5 Absolute pressure distribution (left) and oil spread with dynamic viscosity and maximal velocity (right) at normalized time of 0.22

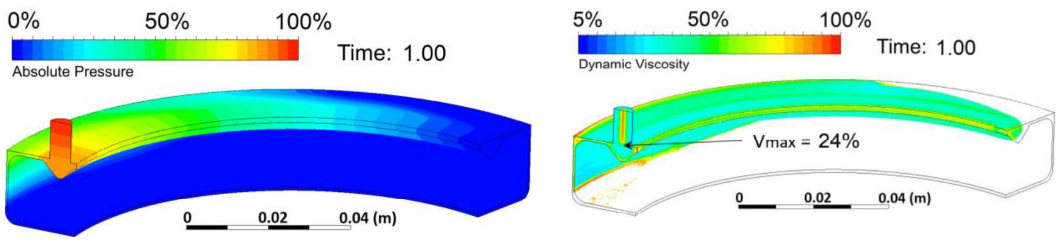

Fig. 6 Absolute pressure distribution (left) and oil spread with dynamic viscosity and maximal velocity (right) at normalized time of 1.00

3.2 Influencing parameter sensitivity analysis

Left side of Fig. 7 presents the effect of the inlet overpressure and oil temperature on the filling time. The results are shown in the diagram of a 3D time-surface plot over the pressure - temperature field. The boundary conditions of the reference filling simulation belong to the minimum point of the surface with normalized filling time of 1.00 at 30 atm overpressure and 80 °C oil temperature. The reason of the shape of the

3D surface is the fact that increasing temperature results in viscosity reduction that makes the silicone oil more fluent. Under the same inlet pressure and under the same time but at higher temperature more amount of oil is pushed into the damper gap. Considering the effect of inlet pressure, higher system pressure at the same temperature and under the same time causes more amount of oil to be pushed into the damper gap.

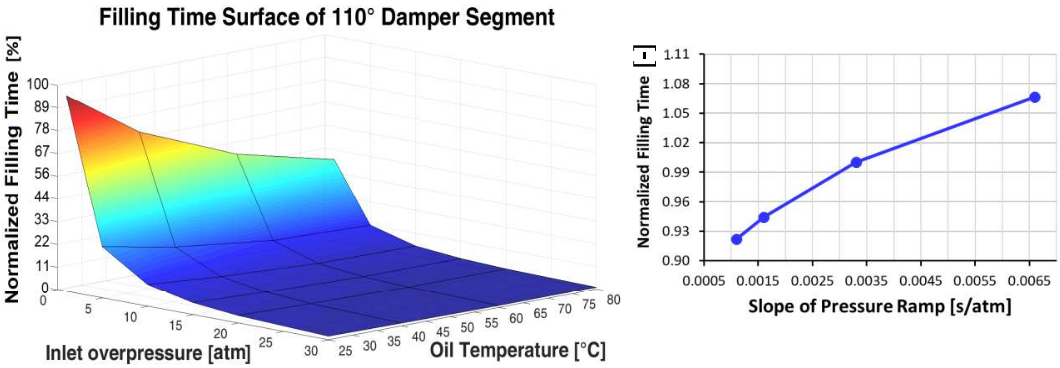

Fig. 7 Parameter sensitivity analysis of the inlet overpressure, oil temperature (left) and the slope of pressure ramp (right) on the filling time

Right side of Fig. 7 shows the influence of the slope of the inlet pressure ramp on the filling time related to simulations with 30 atm inlet overpressure and 80 °C oil temperature. The shortest filling time for the investigated 110° damper segment is reached by applying 30 atm inlet overpressure with 0.0011 s/atm slope of pressure ramp.

As far as the effect of the slope of the pressure ramp is concerned, if shorter time is required for the target inlet pressure to build up (higher pressure gradient), shorter time is needed to the same amount of oil to be pushed into the gap at the same temperature.

Parameter sensitivity analysis has been performed for the inlet overpressure, oil temperature and slope of pressure ramp such a way that only one parameter has been changed (taking roughly the half and roughly the third parts of the reference value) at each investigated scenario. In the last column of Tab. 1, the filling time rates for each investigated scenario have been compared with respect to the maximum filling time. According to these values, inlet overpressure is found to be the most influencing parameter, which effect on the filling time is approximately three times compared to the influence of oil temperature and approximately five times compared to influence of slope of pressure ramp.

Tab. 1 Conditions and results of parameter sensitivity analysis

	Inlet overpressure	**Oil temperature**	**Slope of pressure ramp**	**Normalized filling time to the reference case**	**Filling time rate in the percentage of the maximum one**
Effect of pressure	30 atm	80 °C	0.0033 s/atm	1 [-]	20.83 %
	15 atm	80 °C	0.0033 s/atm	2.8 [-]	58.33 %
	10 atm	80 °C	0.0033 s/atm	4.8 [-]	100 %

Effect of temperature	30 atm	80 °C	0.0033 s/atm	1 [-]	20.83 %
	30 atm	40 °C	0.0033 s/atm	1.39 [-]	28.89 %
	30 atm	25 °C	0.0033 s/atm	1.8 [-]	37.5 %
Effect of slope of pressure ramp	30 atm	80 °C	0.0033 s/atm	1 [-]	20.83 %
	30 atm	80 °C	0.0016 s/atm	0.94 [-]	19.68 %
	30 atm	80 °C	0.0011 s/atm	0.92 [-]	19.21 %

4. CONCLUDING REMARKS

Torsional vibration dampers play an important role in the prevention of fatigue damage of nowadays' high-performance internal combustions engines. The reduction of manufacturing time is a key factor for increasing productivity by improving the filling process with shorter time required for the silicone oil to be filled into the narrow damper gap channels. 3D transient, multiphase, coupled fluid dynamic and heat transfer simulations have been performed with different filling conditions on a damper gap segment with 110° arc angle to provide an insight into the filling process of a specific visco-dampers. Parameter sensitivity analysis has been performed to identify the most influencing boundary condition of the filling time by using numerical simulations. The results of the calculations show that during the filling process, oil's dynamic viscosity has monotonically increasing trend and thus, inflow velocity performs a monotonically decreasing trend, which can be explained by the non-Newtonian and shear-thinning behaviour of the fluid. As far as parameter sensitivity analysis is concerned, inlet overpressure has the highest effect on the filling time while the slope of the pressure ramp influences filling time the least. The shortest filling time is reached by applying 30 atm inlet overpressure with 0.0011 s/atm slope of pressure ramp at 80 °C oil temperature. Nevertheless, high pressures (causing high shear rates) and high temperatures (thermal impact) enhance the degradation process of the oil. As a next step of this work after the validation by measurements, genetic algorithm-based parametric geometry optimization is going to be carried out to identify the appropriate filling conditions and damper gap geometry modifications, which provide the shortest filling time with minimal degradation in the silicone oil.

Acknowledgements

The completion of the present study was supported by the Pro Progressio Foundation. Special thanks to Ákos Horváth at eCon Engineering Ltd. for his technical help in transient CFD simulations.

5. REFERENCES

[1] **Dr. Batrak, Y.**: Torsional Vibration Calculation Issues with Propulsion Systems. ShaftDesigner presentation paper. Available online: http://www.shaftdesigner.com /downloads/PAPER%20TORSIONAL%20VIBRATION%20CALCULATION%20ISSUES%20WITH%20PROPULSION%20SYSTEMS.pdf (accessed on 01.03.2021.)

[2] **Lorenz, H.**: Dynamik Der Kurbelgetriebe: Mit Besonderer Berucksichtigung Der Schiffsmaschinen (1901). Kessinger Publishing, LLC, 2010.

[3] **Frahm, H.**: VDI Zeitschrift, 797, 1902.

[4] **Melville, G.M.**: The Vibration of Steamships. Engineering, 75, 1903.

[5] **Timoshenko, S. P.**: Torsional Vibration of Shafts. Proc. St. Petersburg Polytechnical Institute, 3:55-106, 1905.

[6] **Homik,W.**: Diagnostics, Maintenance and Regeneration of Torsional Vibration Dampers for Crankshafts of Ship Diesel Engines. Polish Maritime Research, 17(1), 2010. p.62-68. DOI: https://doi.org/10.2478/v10012-010-0007-2

[7] **Pfleghaar, J. – Lohmann, B.**: The Electrical Dual Mass Flywheel -an Efficient Active Damping System. IFAC Proceedings Volumes, 46:21, 2013. p.483-488. DOI: https://doi.org/10.3182/20130904-4-JP-2042.00046

[8] **Autohitop**: Diesel engine crankshaft pulley harmonic balancer FOR MITSUBISHI 4D34 MD017116. Available online: https://sc01.alicdn.com/kf/HTB1yxZyfBfM8KJjSZFOq6xr5XXa5/27879/HTB1yxZyfBfM8KJjSZFOq6xr5XXa5.jpg (accessed on 01.03.2021.)

[9] **Geislinger**: Geislinger Vdamp. Product catalog, Geislinger GmbH, 2020. Available online: https://www.geislinger.com/cms_images/products/Vdamp_1.6.pdf (01.03.2021.)

[10] **Feese, T. – Hill, C.**: Prevention of Torsional Vibration Problems in Reciprocating Machinery. Proc. of the 38th Turbomachinery Symposium, 2009. (p.213-238) DOI: https://doi.org/10.21423/R1XP9Z

[11] **Xin, Q.**: Overview of Diesel Engine Applications for Engine System Design – Part 3: Operating and Design Characteristics of Different Applications. SEA Technical Papers, 2011. DOI: https://doi.org/10.4271/2011-01-2180

[12] **Érsek, P.**: Numerische Untersuchung der Auffüllung eines Torsiondämpfers mit Silikonöl, Diplomwork, Knorr-Bremse R&D Center Budapest, Faculty of Mechanical Engineering, Department of Hydrodynamic Systems, Budapest University of Technology and Economics: Budapest, Hungary, 2008.

[13] **ESSS**: Dinámica de Fluidos Computacional: ¿que es? Available online: https://www.esss.co/es/blog/dinamica-de-fluidos-computacional-que-es/ (accessed on 01.03.2021.)

[14] **ANSYS**: ANSYS Fluent Theory Guide, Release 15.0, 2013. Available online: http://www.pmt.usp.br/academic/martoran/notasmodelosgrad/ANSYS%20Fluent%20Theory%20Guide%2015.pdf (accessed on 01.03.2021.).

[15] **Bentley Publishers**: Bosch Electronic Automotive Handbook, 1st ed. Robert Bosch GmbH, 2002. (p. 77) Available online: https://www.academia.edu/8456856/Bosch_automotive_handbook (accessed on 01.03. 2021.)

[16] **Wacker-Chemie**: Wacker Silicone Fluids AK. Product Brochure, Wacker-Chemie GmbH, Available online: https://www.behlke.com/pdf/wacker_silicone_oil.pdf (accessed on 01. 03 2021.)

[17] **Venczel, M. – Bognár, G. – Veress, Á.**: Temperature-Dependent Viscosity Model for Silicone Oil and Its Application in Viscous Dampers. Processes, 9(2):331, 2021. DOI: https://doi.org/10.3390/pr9020331